

Supporting Information

X-ray-activated Ultra-long UVA Persistent Luminescence from Bi-doped Perovskite LaGaO₃ for Photodynamic Activation

Bo-Mei Liu, Yue Lin, Yingchun Liu, Shanqing Zhang, Jing Wang, Hui Zhang,* and Jesse Zhu*

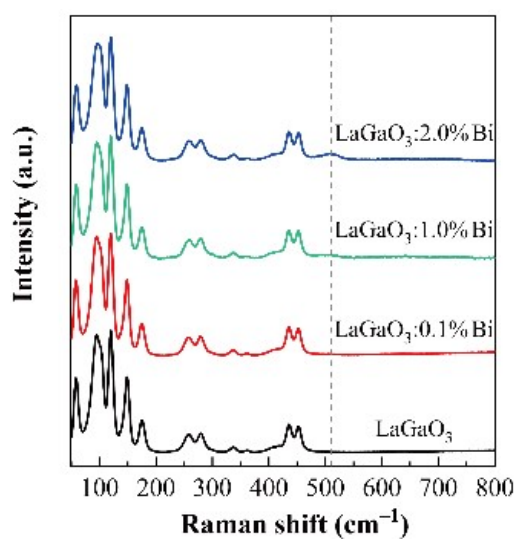


Figure S1. Normalized Raman spectra of undoped and Bi-doped LaGaO₃.

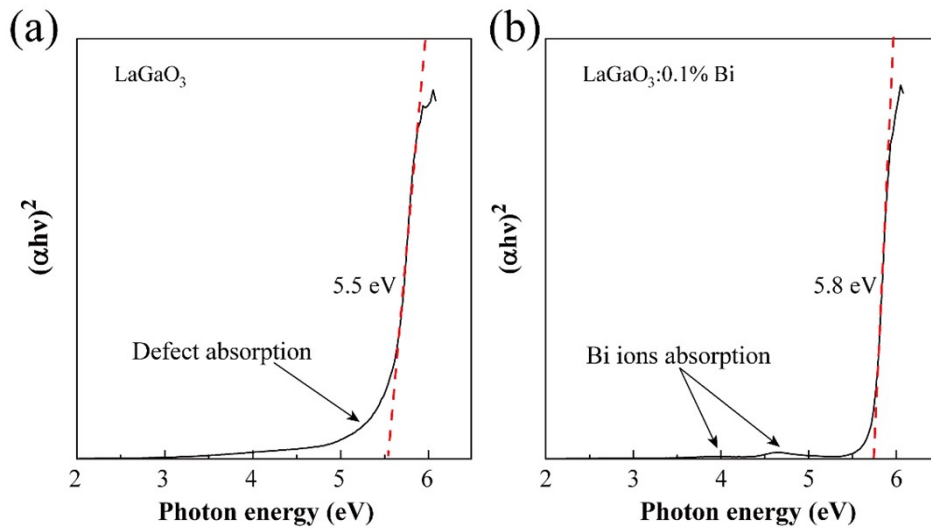


Figure S2. The plot of $(\alpha h\nu)^2$ versus photon energy ($h\nu$) for direct bandgap measurements of (a) LaGaO₃ host and (b) LaGaO₃:0.1%Bi, respectively. Based on the absorption data of **Figure 6a**, the optical band gap has been calculated using the Wood and Tauc model. Note that the apparent absorption tail (Urbach tail) in the LaGaO₃ host comes from energy levels in defective crystalline,¹ which means that the existence of randomly distributed oxygen vacancies inevitably causes a certain degree of structural disorder.

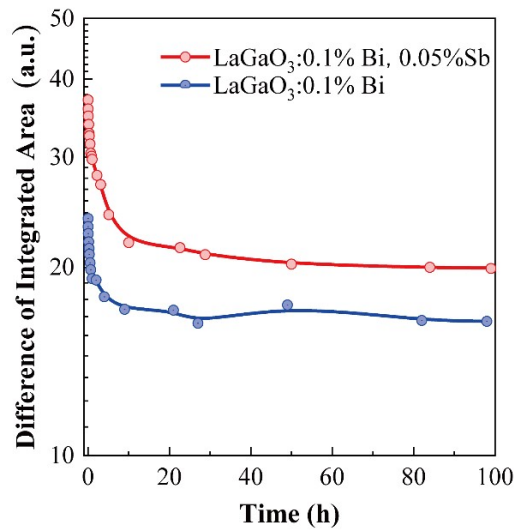


Figure S3. Time dependence of the difference of integrated absorption area ($A_{\text{after irradiation}} - A_{\text{before irradiation}}$) for LaGaO₃: 0.1%Bi based on the data of **Figure 5b**. The sample LaGaO₃:0.1%Bi,0.05%Sb with the best PersL properties were tested at the same time.

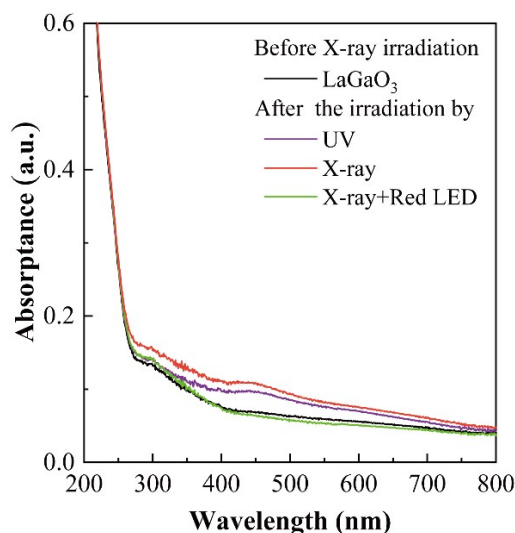


Figure S4. Absorption spectra of the as-obtained LaGaO_3 powder after irradiation by different excitation sources for 5 min. Note: Similar thermal elimination by a red LED light can also be observed in $\text{LaGaO}_3:0.1\% \text{Bi}$.

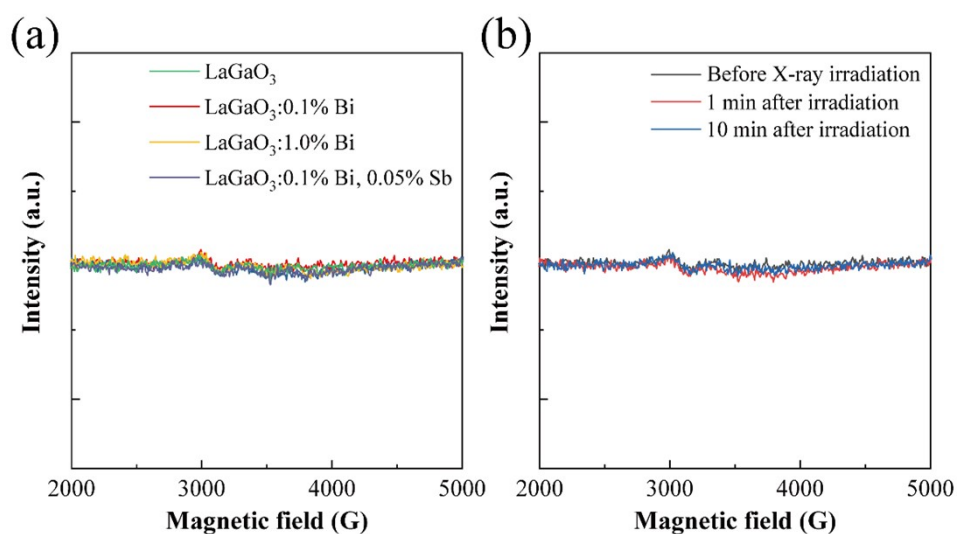


Figure S5. (a) EPR spectra of as-obtained undoped, Bi-doped, and Bi/Sb-codoped LaGaO_3 . (b) EPR spectra of $\text{LaGaO}_3:0.1\% \text{Bi}$ measured at RT before and after X-ray irradiation (5 min). Note that the $\text{LaGaO}_3:\text{Bi}/\text{Sb}$, which has the best PersL performance, also does not show any change during or after the X-ray irradiation, and the small peaks around $G=3300$ in the spectra are due to the existence of trace impurity elements, such as Cr or Mn from the raw materials.

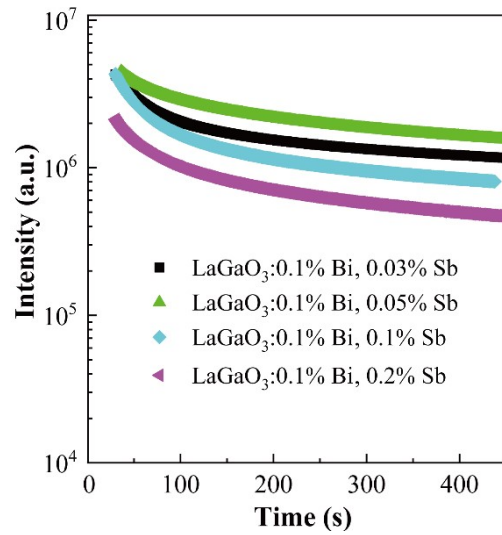


Figure S6. The persistent decay curves of LaGaO₃:0.1%Bi codoped with different Sb monitored at 372 nm after X-ray irradiation for 5 min.

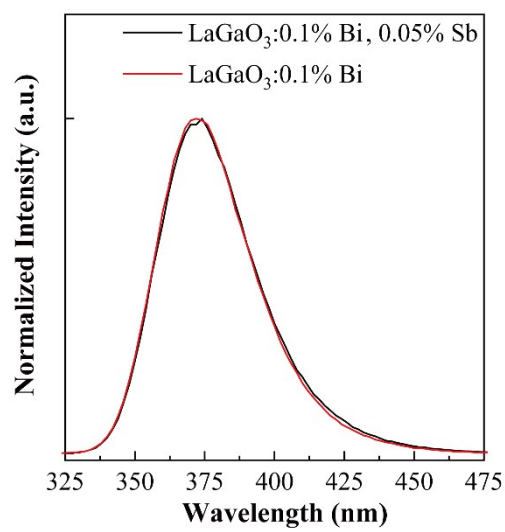


Figure S7. Emission spectra of LaGaO₃:0.1%Bi,0.05%Sb and LaGaO₃:0.1%Bi under the X-ray excitation.

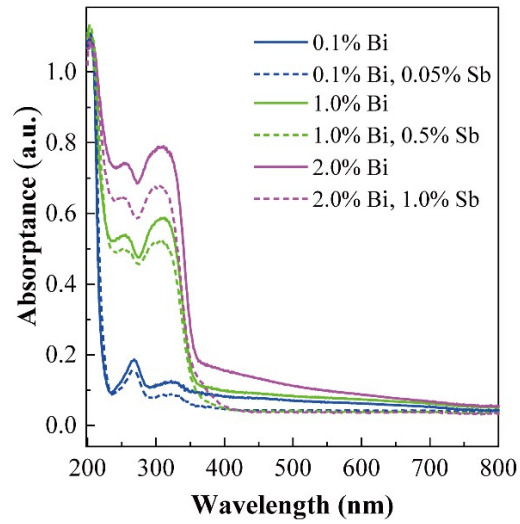


Figure S8. Absorption spectra of the as-synthesized Bi-doped and Bi/Sb codoped LaGaO₃ powder samples.

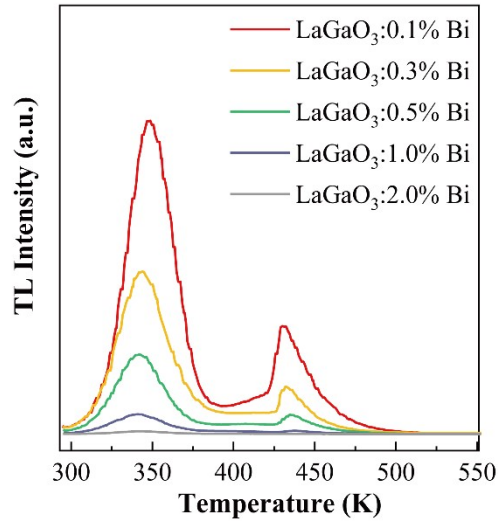


Figure S9. TL glow curves of LaGaO₃:xBi ($x=0.1-2\%$) phosphors at 10 s after X-ray charging for 5 min.

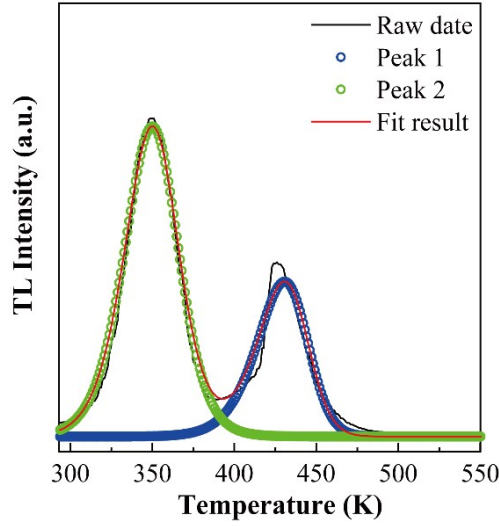


Figure S10. TL curves of LaGaO₃:0.1%Bi,0.05%Sb that were resolved into two bands. The depths of the trap were estimated using the following equation:²

$$I(T) = n_0 S \exp\left(-\frac{E}{kT}\right) \left[(b-1)(S/\beta) \int_{T_0}^T \exp\left(-\frac{E}{kT}\right) dT + 1 \right]$$

Where T is the temperature, n_0 is the concentration of trapped charges at $T = 0$, k is Boltzmann constant, β is the heating rate, E is the activation energy (which means the trap depth), S is frequency, and b is the order of kinetics. The calculated trap depths of the oxygen vacancy are 0.78 eV and 1.12 eV, respectively.

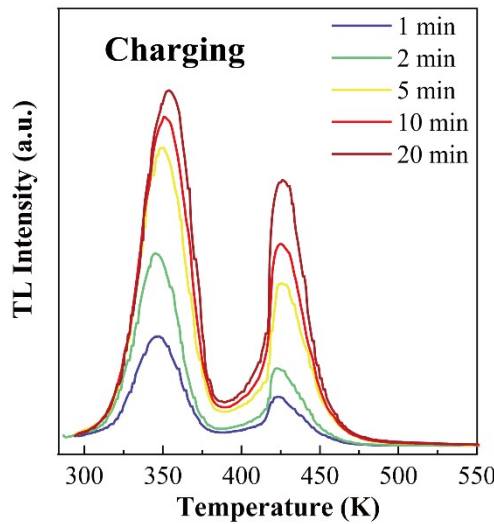


Figure S11. TL curves of the LaGaO₃:0.1%Bi,0.05%Sb sample measured at 10 s after initially irradiated with an X-ray light for 1, 2, 5, 10, and 20 min.

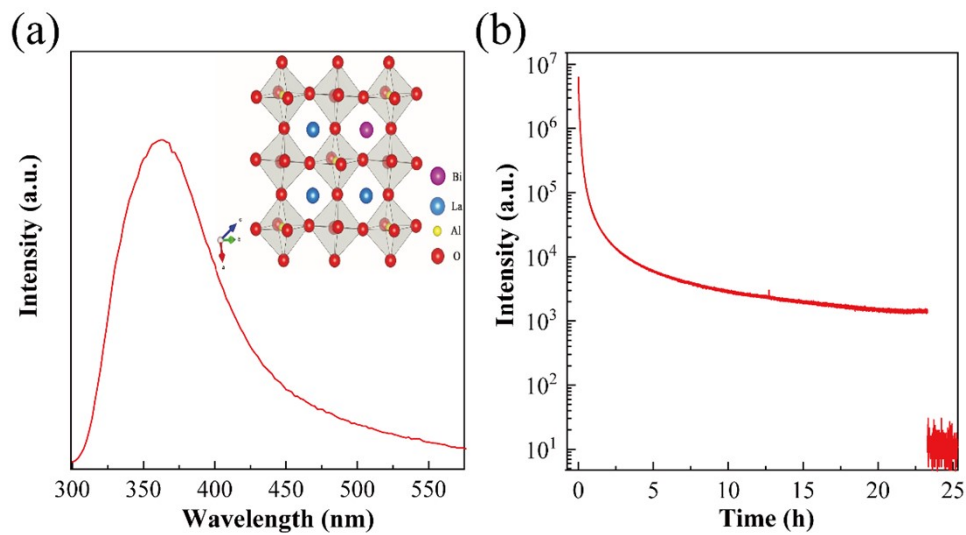


Figure S12. (a) Emission spectrum of $\text{LaAlO}_3:1\%\text{Bi}$ under the X-ray radiation. Inset: schematic diagram of Bi-doped LaAlO_3 structure. (b) PersL decay curve of $\text{LaAlO}_3:1\%\text{Bi}$ monitored at 361 nm after X-ray radiation for 15 min.

References

- [1] Hu, C. Q.; Meng, F. F.; Wen, M.; Gu, Z. Q.; Wang, J. Y.; Fan, X. F.; Zheng, W. T., Relationship between dielectric coefficient and Urbach tail width of hydrogenated amorphous germanium carbon alloy films. *Appl. Phys. Lett.* **2012**, *101* (4), 042109.
- [2] Bos, A. J. J., Theory of thermoluminescence. *Radiat. Meas.* **2006**, *41*, S45-S56.